To cite:
Yuze Wang, Kenichi Soga, Jason T. DeJong, Alexandre J. Kabla. Forthcoming. Effects ofbacterial density on growth rate and characteristics of microbial-induced CaCO3 precipitates:a particle-scale experimental study. ASCE Journal of Geotechnical and GeoenvironmentalEngineering. https://doi.org/10.1016/(ASCE)GT.1943-5606.0002509

Title

Effects of bacterial density on growth rate and characteristics of microbial-induced $CaCO_3$ precipitates: a particle-scale experimental study

Yuze Wang[1]; Kenichi Soga[2]; Jason T. DeJong[3]; Alexandre J. Kabla[4]

Abstract

Microbial-Induced Carbonate Precipitation (MICP) has been explored for more than a decade as a promising soil improvement technique. However, it is still challenging to predict and control the growth rate and characteristics of $CaCO_3$ precipitates, which directly affect the engineering performance of MICP-treated soils. In this study, we employ a microfluidics-based pore scale model to observe the effect of bacterial density on the growth rate and characteristics of $CaCO_3$ precipitates during MICP processes occurring at the sand particle scale. Results show that the precipitation rate of $CaCO_3$ increases with bacterial density in the range between 0.6×10^8 and 5.2×10^8 cells/ml. Bacterial density also affects both the size and number of $CaCO_3$ crystals. A low bacterial density of 0.6×10^8 cells/ml produced 1.1×10^6 crystals/ml with an average crystal volume of 8,000 μm^3, whereas a high bacterial density of 5.2×10^8 cells/ml resulted in more

[1]Assistant Professor, PhD, Department of Ocean Science and Engineering, Southern University of Science and Technology, Shenzhen, People's Republic of China (corresponding author). E-mail: wangyz@sustech.edu.cn, ORCID: 0000-0003-3085-5299

[2]Chancellor's Professor, PhD, FREng, FICE, Department of Civil and Environmental Engineering, University of California, Berkeley, USA, soga@berkeley.edu, ORCID: 0000-0001-5418-7892

[3] Professor, PhD, Department of Civil and Environmental Engineering, University of California, Davis, USA, jdejong@ucdavis.edu, ORCID: 0000-0002-9809-955X

[4] Reader, PhD, Department of Engineering, University of Cambridge, Cambridge, UK, ajk61@cam.ac.uk, ORCID: 0000-0002-0280-3531

To cite:
Yuze Wang, Kenichi Soga, Jason T. DeJong, Alexandre J. Kabla. Forthcoming. Effects ofbacterial density on growth rate and characteristics of microbial-induced CaCO3 precipitates:a particle-scale experimental study. ASCE Journal of Geotechnical and GeoenvironmentalEngineering. https://doi.org/10.1016/(ASCE)GT.1943-5606.0002509

crystals (2.0×10^7 crystals/ml) but with a smaller average crystal volume of 450 μm^3. The produced $CaCO_3$ crystals were stable when the bacterial density was 0.6×10^8 cells/ml. When the bacterial density was 4-10 times higher, the crystals were first unstable and then transformed into more stable $CaCO_3$ crystals. This suggests that bacterial density should be an important consideration in the design of MICP protocols.

Keywords

Soil stabilization, ground improvement, particle-scale behaviour, microscopy, time dependence, mineralogy, Microbial-Induced $CaCO_3$ Precipitation

INTRODUCTION

Microbial-Induced Calcium Carbonate Precipitation (MICP) has been extensively investigated for applications such as ground improvement, soil liquefaction mitigation, dam safety control, prevention of soil erosion, and slope stabilisation (van Paassen, 2009; DeJong *et al.*, 2013; Martinez *et al.*, 2013; Montoya *et al.*, 2013; Jiang *et al.*, 2017). The $CaCO_3$ precipitates fill soil pores and bond soil particles, which consequently increase the strength and stiffness, and reduce the permeability of the soil matrix (Stocks-Fischer *et al.*, 1999; DeJong *et al.*, 2006). Several types of bacterial activities including ureolysis, denitrification and sulfate reduction can result in MICP (DeJong *et al.*, 2010), and among those the ureolysis-based process has been most widely studied. Ureolysis-driven MICP involves urea hydrolysis by the urease enzyme produced by active microorganisms (Equation 1), resulting in the generation of calcium carbonate ($CaCO_3$) in the soil matrix (Equation 2).

$$CO(NH_2)_2 + 2H_2O \xrightarrow{Urease} 2NH_4^+ + CO_3^{2-} \quad (1)$$

$$Ca^{2+} + CO_3^{2-} \rightarrow CaCO_3(s) \quad (2)$$

To cite:
Yuze Wang, Kenichi Soga, Jason T. DeJong, Alexandre J. Kabla. Forthcoming. Effects ofbacterial density on growth rate and characteristics of microbial-induced CaCO3 precipitates:a particle-scale experimental study. ASCE Journal of Geotechnical and GeoenvironmentalEngineering. https://doi.org/10.1016/(ASCE)GT.1943-5606.0002509

Ureolysis and $CaCO_3$ precipitation are the two key processes involved in the ureolysis-driven MICP process. Understanding the kinetics of these two processes is essential for designing MICP protocols. The kinetics of ureolysis is normally assessed by the increase in solution conductivity due to the hydrolysis of urea (Whiffin *et al.*, 2007; Lauchnor *et al.*, 2015). The kinetics of $CaCO_3$ precipitation can be assessed by the decrease in Ca^{2+} concentration (Stocks-Fischer *et al.*, 1999). Recently, the kinetics of $CaCO_3$ at the crystal size level have also been studied by using optical microscopes to observe $CaCO_3$ crystals produced in liquid medium in petri dishes (Zhang *et al.*, 2018), on glass slides (Wang *et al.* 2019b) or in microfluidic chips (Wang *et al.* 2019a,b; Kim *et al.*, 2020), as well as crystals produced on solid agar pads (Zhang *et al.*, 2018). Crystals grew steadily to diameters of 20 μm and 50 μm within 40 minutes when MICP occurred in a liquid medium placed in a petri dish or on an agar pad containing Ca^{2+} urea, respectively (Zhang *et al.*, 2018). In comparison, the use of a microfluidic-based porous model is considered to be a more appropriate approach to study the kinetics of MICP as it more closely mimics real MICP conditions occurring in the pore fluid of a porous soil matrix where bacterial cells move freely and the cementation solution can be injected multiple times (Wang *et al.*, 2019 a,b).

In addition to the $CaCO_3$ precipitation kinetics, the properties of $CaCO_3$ precipitates also need to be considered in a MICP protocol design. Larger crystals that bond soil particles more sufficiently may increase soil strength more effectively (Cheng *et al.*, 2017). By conducting soil column experiments and by using a scanning electronic microscopy to scan the samples after MICP treatment, it was found that the concentration of cementation solution and ureolysis activity affected the size and number of $CaCO_3$ crystals after MICP treatment (Al Qabany & Soga, 2013; Cheng *et al.*, 2017). Al Qabany & Soga (2013) found that when the total treatment duration and the total amount of cementation solution were constant, the use of higher concentrations of cementation

To cite:
Yuze Wang, Kenichi Soga, Jason T. DeJong, Alexandre J. Kabla. Forthcoming. Effects ofbacterial density on growth rate and characteristics of microbial-induced CaCO3 precipitates:a particle-scale experimental study. ASCE Journal of Geotechnical and GeoenvironmentalEngineering. https://doi.org/10.1016/(ASCE)GT.1943-5606.0002509

solution produced larger $CaCO_3$ crystals. Cheng *et al.* (2017) showed that higher bacterial activities tend to produce smaller $CaCO_3$ crystals at the end of MICP treatment.

Because $CaCO_3$ crystals were only observed after MICP treatment by using a scanning electronic microscopy (Al Qabany & Soga, 2013; Cheng *et al.*, 2017), the kinetics and characteristics of microbial-induced $CaCO_3$ precipitation were not fully understood. Wang *et al.* (2019a) designed and fabricated a microfluidic chip etched with porous models and used it to observe the MICP process under conditions that resemble soil assemblies. The advantage of this method is that the density of bacteria and the main parameters of $CaCO_3$ crystals such as size, shape and number can be quantified during the whole MICP process (Wang *et al.*, 2019 a,b). Wang *et al.* (2019b) found that when the bacterial activity and concentration of cementation solution were the same, longer injection intervals (23-25 hours compared to 3-5 hours) produced larger and fewer $CaCO_3$ crystals. This was because when the interval was longer, the smaller and less stable crystals dissolved while the larger and more stable crystals continued to grow (Wang *et al.*, 2019b).

Therefore, it is essential to investigate the processes of MICP rather than only the MICP properties after MICP treatment to have a better understanding of the kinetics and properties of MICP. Due to the fact that bacterial density has a direct effect on the ureolysis activity (Lauchnor *et al.*, 2015) and a large range of bacterial densities have been used in MICP studies (Al Qabany *et al.*, 2012; Cheng *et al.*, 2017), it is essential to know the quantity and activity of the bacteria injected into the soil to design robust MICP treatment protocols. In this study, microfluidic experiments were conducted to observe both the growth kinetics and characteristics of microbial-induced $CaCO_3$ crystals under conditions where the bacterial densities varied. The test results were used to investigate

To cite:
Yuze Wang, Kenichi Soga, Jason T. DeJong, Alexandre J. Kabla. Forthcoming. Effects ofbacterial density on growth rate and characteristics of microbial-induced CaCO3 precipitates:a particle-scale experimental study. ASCE Journal of Geotechnical and GeoenvironmentalEngineering. https://doi.org/10.1016/(ASCE)GT.1943-5606.0002509

the effects of bacterial density on the kinetics and characteristics of $CaCO_3$ precipitation and to provide suggestions for MICP treatment protocols.

MATERIALS AND METHODS

Microfluidic chip experimental setup and data acquisition

The microfluidic chip used in this study was designed based on a cross-sectional image of a solidified and sectioned 3D Ottawa 30–50 sandy soil specimen and the fabrication of the microfluidic chip was conducted following the standard photolithography techniques by using polydimethylsiloxane (PDMS) and glass. The design and fabrication methods of the microfluidic chips were discussed in Wang *et al.* (2019a). The experimental setup is shown in Figure 1.

During the experiments, all images were acquired with an Axio Observer Z1 research microscope. The microscope is a phase-contract microscope and is equipped with an automated stage (Prior Scientific Instrument), a grayscale camera (Hamamatsu C11440-22CU), and a light source connected to a computer and controlled by Zeiss AxioVision image analysis software. Images were captured using phase field illumination and 10× inverted objectives (with image resolutions of 0.65 μm/pixel). Under the phase-contract microscope, bacterial cells appeared as black dots, the $CaCO_3$ precipitates appeared as white dots, and the microfluidic chip appeared as light to dark grey background (Wang et al., 2019b).

Preparation of bacterial suspension and cementation solution

Sporosarcina pasteurii (DSM 33), a ureolytic bacterial strain, was used in the experiments. Bacterial cells from the glycerol stock (Wang *et al.*, 2019b) were grown in ATCC 1376 NH_4-YE agar medium (20 g/L yeast extract, 10 g/L ammonium sulphate, 20 g/L agar, and 0.13 M Tris base) for 48 hours at 30°C. Subsequently, several colonies on

To cite:
Yuze Wang, Kenichi Soga, Jason T. DeJong, Alexandre J. Kabla. Forthcoming. Effects ofbacterial density on growth rate and characteristics of microbial-induced CaCO3 precipitates:a particle-scale experimental study. ASCE Journal of Geotechnical and GeoenvironmentalEngineering. https://doi.org/10.1016/(ASCE)GT.1943-5606.0002509

the agar plate were transferred to a NH_4-YE liquid medium containing the same components without agar and cultivated in a shaking incubator for 24 hours at 30°C and at a shaking rate of 200 rotations per minute (rpm) to obtain a bacterial suspension with an optical density measured at a wavelength of 600 nm (OD_{600}) of around 3.0. A more detailed description of the preparation of the bacterial suspension can be found in Wang *et al.* (2019b). The cementation solution contained 0.25 mol/L of $CaCl_2$, 0.375 mol/L of urea and 3 g/L of nutrient broth.

Staged injection procedure of cementation solution to produce $CaCO_3$ precipitates

A staged injection procedure was applied to the MICP treatment process. After bacterial injection into a microfluidic chip and the subsequent 2 hour bacterial settling period, 1.25 pore volumes (PV) of cementation solution was injected into the microfluidic chip at an injection flow rate of 5.6 PV/hr. Subsequent injections of cementation solution were conducted at 24-hour intervals after the previous injection. In total, 12 injections of cementations solution were applied. The injection volume of cementation solution, the flow rate, and the number of injections of cementation solution were chosen based on findings presented in Wang *et al.* (2019a, b). Time-series images were captured at 15 minutes intervals after the completion of each of the cementation solution injections. The main experimental parameters in these protocols are summarised in Table 1.

Quantification of bacterial density and activity

Bacterial suspensions with five different densities were prepared to correlate with bacterial optical density. The OD_{600} was measured to quantify the bacterial density before the injection of 1.5 PV into each of five microfluidic chips at an injection flow rate of 56 PV/h. The bacterial suspensions were prepared by diluting the bacterial suspension with OD_{600} of 3.0 using autoclaved NH_4-YE liquid medium at volume proportions V_bacterial suspension : V_NH_4-YE liquid medium of 1:14, 1:5, 1:2, 2:1 and 1:0. NH_4-YE liquid

To cite:
Yuze Wang, Kenichi Soga, Jason T. DeJong, Alexandre J. Kabla. Forthcoming. Effects ofbacterial density on growth rate and characteristics of microbial-induced CaCO3 precipitates:a particle-scale experimental study. ASCE Journal of Geotechnical and GeoenvironmentalEngineering. https://doi.org/10.1016/(ASCE)GT.1943-5606.0002509

medium provides nutrients for bacterial activity. Therefore, to avoid bacterial starvation, autoclaved NH_4-YE liquid medium instead of Deionized water was used to dilute the bacterial suspension from OD_{600} of 3.0 to prepare bacterial suspensions at lower densities. It should be noted that due to the difference in dilution ratios, the amount of nutrients provided to the bacterial cells varies when the bacterial densities are different, and this difference was not considered in this study. Injecting 1.5 PV of bacterial suspension at a flow rate of 56 PV/h resulted in a homogeneous distribution of bacteria after injection (Wang *et al.*, 2019a). The bacterial density was quantified based on the images taken at the centre of the microfluidic chips. Bacteria were given 10 mins to settle to the bottom zone of the microfluidic chip before obtaining accurate microscope images since the microscope focal length depth range was 17 µm, whereas the depth of the microfluidic chip was 50 µm. The bacterial cells doubled in number in about 2 hours due to *in situ* growth during bacterial settling (Wang *et al.*, 2019a). The effect of bacterial growth on the bacterial density changed during the first 10 minutes, but this was neglected due the short period. Because bacterial size affects the reading of OD_{600} value (Zapata & Ramirez-Arcos, 2015), the sizes of the bacteria were also measured to obtain the average bacterial size.

To examine the effect of bacterial density on the rate of ureolysis, a series of batch tests was conducted by varying the bacterial densities in bacteria-urea mixtures. The hydrolysis rate was measured using the conductivity method described by Whiffin *et al.* (2007). The urea concentration in the bacteria-urea mixtures was 1.0 M before the hydrolysis of urea occurred. The bacterial densities in the bacteria-urea mixtures were equivalent to OD_{600} of 0.1, 0.25, 0.46, 0.75, 1.035, 1.38 and 1.73. The conductivity of the mixed content was assessed by using a conductivity meter (FiveGo, Meter Toledo) immediately after the mixing and five minutes after mixing. The ureolysis rate was calculated using Equation 3 (Whiffin *et al.*, 2007). Measurements were

To cite:
Yuze Wang, Kenichi Soga, Jason T. DeJong, Alexandre J. Kabla. Forthcoming. Effects ofbacterial density on growth rate and characteristics of microbial-induced CaCO3 precipitates:a particle-scale experimental study. ASCE Journal of Geotechnical and GeoenvironmentalEngineering. https://doi.org/10.1016/(ASCE)GT.1943-5606.0002509

performed in triplicates for each of the different media tested, with data presented as mean ± standard error.

$$Ureolysis\ rate(mM/h) = \frac{\Delta Conductivity(\mu S/cm)}{\Delta t(\min)} \times (10^{-3} \times 11.11)(mM/(\mu S/cm)) \times 60(\min/h) \quad (3)$$

Quantification of crystal growth rate, size, and quantity

Several methods were used to quantify $CaCO_3$ crystal characteristics. Mean intensity values of the images were analysed using Zeiss Axio Vision image analysis software and plotted against time to show how the relative areas occupied by the precipitates changed with time. The image intensities could not represent the total crystal volume produced because two-dimensional images cannot capture the entire information of the three-dimensional crystals but could represent the change in crystal properties with time. In addition, crystal diameter has previously been used to quantify the size of $CaCO_3$ crystals (Zhang *et al.*, 2018). During the initial growth stage, most crystals were hemispheres and grew on the surface of the microfluidic channel (Wang *et al.*, 2019; Kim *et al.*, 2020). Therefore, in this study, the volumes of individual crystals were calculated based on their measured diameters. In addition, numbers of crystals were also counted to quantify crystal number.

RESULTS AND DISCUSSION

Bacterial density and bacterial optical density

The bacterial densities of five bacterial suspensions (cells/ml) were correlated with their initial OD_{600} values to quantify the bacterial density used. Microscope images were taken at the centre of five microfluidic chips containing bacterial suspensions with the initial OD_{600} of 0.2, 0.5, 1.0, 2.0 and 3.0 at 10 minutes after the injection of bacterial suspensions (shown in Figure 2a). Bacterial densities correlated with the initial OD_{600} values of the bacterial suspensions and the results are shown in Figure 2b. A blank sample with no bacterial cells in the bacterial nutrient liquid was used as a baseline

against which the OD_{600} was defined as zero. The data shows that bacterial density and OD_{600} are linearly correlated as:

$$Bacterial\ density\ (cells\ per\ ml) = OD_{600} \times 4 \times 10^8 \quad (4)$$

The R^2 values of the all three linear regression lines in Figure 2b are higher than 0.99.

Because bacterial cell size affects the optical density of a bacterial suspension, magnified images of the microfluidic chips containing bacterial suspensions in this study and a previous study (Wang *et al.*, 2019a) are presented to show how the difference in bacterial cell size would affect the optical density of the bacterial suspension (Figure 2c and d). The sizes of bacterial cells in this study are about 3 μm, whereas the ones in Wang *et al.* (2019a) are about 10 μm. Consequently, at the same optical density, the bacterial density in this study is about 3 times higher of that in Wang *et al.* (2019a). Because of the difference in bacterial size, the ureolysis rate may vary when the bacterial optical densities are the same. Therefore, in this study, the bacterial cells were obtained from one batch of bacterial suspension, where the sizes of bacterial cells were relatively consistent, and the bacterial densities were modified to obtain a variety of bacterial activities in terms of ureolysis rate.

Bacterial density during MICP processes

Three MICP processes using different bacterial densities were conducted in microfluidic experiments. Optical densities of the bacterial suspensions were measured prior to the injections of bacterial suspensions. Bacterial densities (in cells per ml) of the bacterial suspensions were quantified (i) after injection of bacterial suspension, (ii) after 2 hours of settling, and (iii) after injection of the cementation solution. The results are presented in Table 2. The corresponding microscope images and results are presented in Figures 3a and 3b, respectively. When the initial bacterial densities were $(0.96\pm0.03)\times10^8$, $(3.92\pm0.29)\times10^8$ and $(11.90\pm0.61)\times10^8$ cells/ml, after 2 hours of settling the bacterial

To cite:
Yuze Wang, Kenichi Soga, Jason T. DeJong, Alexandre J. Kabla. Forthcoming. Effects ofbacterial density on growth rate and characteristics of microbial-induced CaCO3 precipitates:a particle-scale experimental study. ASCE Journal of Geotechnical and GeoenvironmentalEngineering. https://doi.org/10.1016/(ASCE)GT.1943-5606.0002509

densities increased to $(1.92\pm0.13)\times10^8$, $(6.09\pm0.34)\times10^8$ and $(15.4\pm0.88)\times10^8$ cells/ml, respectively, due to bacterial growth *in situ* (Table 2 and Figure 3b). The highest growth rate was obtained when the initial bacterial density was low (about 1×10^8 cells/ml); the cell density became about 2 times higher than the initial density after 2 hours. When the initial bacterial density was high (about 4×10^8 cells/ml), the bacteria growth rate was about 1.5 times higher than the initial density. When the initial bacterial density was very high (about 12×10^8 cells/ml), the growth rate was about 1.25 times higher than the initial densities, which was the lowest among the three cases. The difference in bacterial growth rate might be because the relative abundance of nutrients available to the bacterial population varied depending on the initial bacterial density, with individual bacteria in more concentrated bacterial suspensions being exposed to a smaller share of the total nutrients available.

After the injection of cementation solution, about 30% of the bacteria (approximately 0.6×10^8, 2.0×10^8 and 5.2×10^8 cells/ml for the three cases) remained attached to the inner surface of the microfluidic chip compared to the number of bacteria present after bacterial settling (Table 2 and Figure 3b). The actual bacterial density is expected to be higher than these values since bacteria aggregation also occurred after the cementation solution injection, especially when the bacterial density was high, and the number of bacteria present in bacteria aggregates could not be counted. The percentage of bacteria remaining (30%) is lower than that in Wang *et al.* (2019a), which was 45% after the first injection of cementation solution. This might be because the bacterial settling time was 2 hours in this study, which is lower than the settling time used in Wang *et al.* (2019a), which was 24 hours. In this study, the 2 hours bacterial settling time was used to study the effect of bacterial density on the kinetics and characteristics of MICP.

To cite:
Yuze Wang, Kenichi Soga, Jason T. DeJong, Alexandre J. Kabla. Forthcoming. Effects ofbacterial density on growth rate and characteristics of microbial-induced CaCO3 precipitates:a particle-scale experimental study. ASCE Journal of Geotechnical and GeoenvironmentalEngineering. https://doi.org/10.1016/(ASCE)GT.1943-5606.0002509

Bacteria's attachment to and detachment from soil particles are affected by several factors such as the surface properties of soil particles, the behaviour of bacteria and pore fluidic composition (Dunne, 2002; Chen et al., 2010; Liu et al., 2011; Persat et al., 2015). To simulate the surface properties of real sandy soils, the PDMS surface was treated to be hydrophilic and negatively charged and the bacterial suspension was prepared in the same condition as it could be applied in the field (Wang et al., 2019b). In addition, upscaling experiments conducted by both microfluidic chip tests and soil column tests also showed consistent results observed at both scales (Wang et al., 2020, Wang, 2019). Deionised water was used to saturate the microfluidic chips in these studies, which is the same as the conditions reported in many MICP papers, but they did not consider the effects of parameters such as pH, chemicals, temperature and dissolved oxygen of the pore fluid on the bacteria-soil interactions in real soils. The bacteria-soil interactions under the conditions that simulate real MICP-treated subsurfaces and natural environment by varying the composition of the pore fluid and environmental factors can be considered in future studies. It should be noted that there are both live and dead bacteria in the bacterial suspensions, and the current method presented in this study cannot be used to distinguish between dead and live bacterial cells. Other experimental methods are needed to investigate the effects of live and dead bacteria on the formation of calcium carbonate precipitation.

Ureolysis rate

To examine the effect of bacterial density on the rate of ureolysis, a batch test was conducted in which the bacterial densities in bacteria-urea mixtures were varied and the hydrolysis rate was measured by using the conductivity method described by Whiffin *et al.* (2007). The urea concentration in the bacteria-urea mixture was 1.0 M before the hydrolysis of urea occurred (Figure 4). Bacterial density in the range of 0.5×10^8 to 4×10^8 cells/ml increased the ureolysis rate (Figure 4), while for bacterial densities exceeding

To cite:
Yuze Wang, Kenichi Soga, Jason T. DeJong, Alexandre J. Kabla. Forthcoming. Effects ofbacterial density on growth rate and characteristics of microbial-induced CaCO3 precipitates:a particle-scale experimental study. ASCE Journal of Geotechnical and GeoenvironmentalEngineering. https://doi.org/10.1016/(ASCE)GT.1943-5606.0002509

around 4×10^8 cells/ml the ureolysis rate no longer increased with bacterial density. The linear increase in ureolysis rate associated with bacterial densities in the range of 1×10^7 - 2×10^8 cells/ml is consistent with the results obtained by Lauchnor *et al.* (2015). The highest previously reported ureolysis rate was measured when bacterial density was 2×10^8 cells/ml (Stocks-Fischer et al., 1999; Lauchnor *et al.* 2015). However, the current study shows that, when the bacterial density exceeds 5×10^8 cells/ml, the ureolysis rate does not linearly increase with bacterial density, which might be because there could be insufficient nutrients available to sustain bacterial growth at such high bacterial densities.

Bulk precipitation rate of $CaCO_3$

The precipitation of $CaCO_3$ with time in the three microfluidic experiments is shown in the images taken at 0.5 hr, 1 hr, 3 hr and 24 hr after the cementation solution injection in Figure 5a. Changes in image intensity with time in the three cases with varied bacterial densities are shown in Figure 5b. The areas in the microfluidic chips occupied by $CaCO_3$ crystals were also different, where a higher bacterial density (e.g. 5.2×10^8 cells/ml) resulted in crystals occupying a larger area, as shown by the difference in the image intensities.

We hypothesized that the point when image intensity no longer increases indicated the completion of the $CaCO_3$ precipitation process. The time at which the image intensity stopped increasing in these three cases also varied. The time required for $CaCO_3$ precipitation to complete decreased from 15 hrs to 1.5 hrs when the bacterial densities increased from 0.6×10^8 to 5.2×10^8 cells/ml. The correlation between precipitation rate and bacterial density is shown in Figure 5b. Bacterial density positively affects the overall $CaCO_3$ precipitation rate, and the average precipitation rate in the three cases are 0.016, 0.083 and 0.16 M/h when the corresponding bacterial densities were 0.6×10^8, 2.0×10^8, and 5.2×10^8 cells/ml, respectively.

To cite:
Yuze Wang, Kenichi Soga, Jason T. DeJong, Alexandre J. Kabla. Forthcoming. Effects ofbacterial density on growth rate and characteristics of microbial-induced CaCO3 precipitates:a particle-scale experimental study. ASCE Journal of Geotechnical and GeoenvironmentalEngineering. https://doi.org/10.1016/(ASCE)GT.1943-5606.0002509

310

311 **Precipitation rates and sizes of individual $CaCO_3$ crystals**

312 Individual $CaCO_3$ crystals are shown in the magnified images of one of the middle pores
313 inside the microfluidic chips at 0.5, 1, 1.5, 2, 6, 15 and 24 hours after the first cementation
314 injection in Figure 6a. The average crystal volumes calculated based on the measured
315 diameters at an interval of 15 minutes during the first 1.5 hours and over the 24 hours
316 are plotted against time in Figures 6b and 6c, respectively. The average crystal volume
317 data show that, unlike the effect of bacterial density on the overall precipitation rate of
318 $CaCO_3$, bacterial density has no effect on the growth rate of individual $CaCO_3$ crystals.
319 During the first 1.5 hours after the injection of cementation solution, the crystals grew
320 steadily at the same growth rate even though the bacterial density varied (Figure 6b).
321 The crystals grew to be about 380 ± 40 μm^3 by 1.5 hours for all the three bacterial density
322 cases (Figure 6b).

323

324 However, the time required for the crystals to finish growing and the final size varied in
325 the three cases. In the low bacterial density case (0.6×10^8 cells/ml case), crystal growth
326 continued over 15 hours, which was the longest among the three cases. The average
327 size of the crystals at the completion of crystal growth was about 8000 μm^3, which was
328 the largest among the three cases. For the high bacterial density case (2.0×10^8 cells/ml
329 case), the overall precipitation rate indicated that the precipitation process completed by
330 around 3 hours (Figure 5b), while individual crystal precipitation rates shows that the
331 process completed by around 10 hours (Figure 6c). The growth of the crystals between
332 3 and 10 hours is largely due to the dilution of unstable crystals (circled in Figure 6a),
333 which contributed to the growth of larger crystals. This result is consistent with the
334 observation obtained in Wang *et al.* (2019b). The final average size of the crystals was
335 1800 μm^3 after 10 hours. For the very high bacterial density case (5.2×10^8 cells/ml),

To cite:
Yuze Wang, Kenichi Soga, Jason T. DeJong, Alexandre J. Kabla. Forthcoming. Effects ofbacterial density on growth rate and characteristics of microbial-induced CaCO3 precipitates:a particle-scale experimental study. ASCE Journal of Geotechnical and GeoenvironmentalEngineering. https://doi.org/10.1016/(ASCE)GT.1943-5606.0002509

crystals stopped growing by 1.5 hours and the final average size of the crystals was about 400 μm^3 after 1.5 hours (Figure 6a and 6b).

Crystal quantity

The quantity of crystals formed when the bacterial density was very high (5.2×10^8 cells/ml) is compared to when the bacterial density was high (2.0×10^8 cells/ml) in Figure 5a and 6a. When the bacterial density was low (0.6×10^8 cells/ml), the number of crystals was the lowest among the three cases (Figure 5a and 6a). To illustrate this, the number of crystals in the three cases at each instance when imaging was taken within the first 24 hours were quantified (Figure 7). The $CaCO_3$ crystal concentration represents the quantity of $CaCO_3$ crystals formed per unit volume (i.e. 1 ml). A higher bacterial density resulted in a larger quantity of crystals. When bacterial density was 0.6×10^8, 2×10^8 and 5.2×10^8 cells/ml, the concentration of crystals formed was about 1.5×10^6, 7×10^6, and 2.1×10^7 per ml, respectively, at 24 hours after the cementation solution injection. Bacterial density positively correlated with the number of crystals and the overall crystal growth rate.

The change in the number of crystals with time differed among the three cases. When the bacterial density was 0.5×10^8 cells/ml, the number of crystals increased to around 2×10^6 per ml soon after the cementation solution injection. When the bacterial density was 2.0×10^8 cells/ml, the number of crystals increased to around 14×10^6 per ml by 3 hours and then decreased to around 7×10^6 per ml by around 10 hours. The decrease in crystal number was due to the dissolution of unstable crystal forms. When the bacterial density was 5.2×10^8 cells/ml, the number of crystals increased to around 20×10^6 per ml by around 3 hours after the cementation solution injection. Dissolution of crystals occurred but was not as obvious compared to when the case when the bacterial density was 2.0×10^8 cells/ml.

To cite:
Yuze Wang, Kenichi Soga, Jason T. DeJong, Alexandre J. Kabla. Forthcoming. Effects ofbacterial density on growth rate and characteristics of microbial-induced CaCO3 precipitates:a particle-scale experimental study. ASCE Journal of Geotechnical and GeoenvironmentalEngineering. https://doi.org/10.1016/(ASCE)GT.1943-5606.0002509

363

364 **Crystal type and dissolution**

365 It was found that less stable and smaller $CaCO_3$ crystals may dissolve at the expense of
366 growth of more stable and larger $CaCO_3$ crystals (Wang et al., 2019b). As shown in
367 Figures 6 and 7, crystal dissolution occurred in the cases when the bacterial density was
368 either 2×10^8 cells/ml or 5.2×10^8 cells/ml, but not when the bacterial density was 0.6×10^8
369 cells/ml. To investigate the effects of bacterial density on the dissolution of the crystals,
370 microscope images captured at different instances each of the 12 cementation solution
371 injections are shown in Figure 8. Figures 8a and 8b show the images taken between 0
372 and 24 hours after the first and the second injections of cementation solution,
373 respectively. Figure 8c shows the images taken at 24 hours after the 3rd, 6th, 9th and 12th
374 injections of cementation solution.

375

376 When the bacterial density was low (0.5×10^8 cells/ml in this study), the crystals that were
377 present 24 hours after the cementation solution injection were mainly prismatic,
378 suggesting that the crystals are calcite (Al Qabany *et al.,* 2012; Zhao *et al.,* 2014). These
379 crystals continued growing during the intervals between injections of cementation
380 solution. When the bacterial density was high (2×10^8 cells/ml), the crystals which formed
381 after injections of cementation solution were mainly spherical or prismatic. The spherical
382 crystals were relatively unstable and often dissolved, while the prismatic crystals stayed
383 stable. Both the shape and relative solubility of these crystals are consistent with those
384 of calcite and vaterite, respectively (Wang et al., 2019b). When the bacterial density was
385 very high (5.2×10^8 cells/ml), bacteria aggregates were observed after the first
386 cementation solution injection. Irregular-shaped crystals formed on top of them (Figure
387 8c). Spherical crystals were also observed. Although this form of $CaCO_3$ precipitates
388 remained present after several initial injections of cementation solution (Figures 8c), they
389 were eventually replaced by more stable forms of $CaCO_3$ crystals. This suggests that

To cite:
Yuze Wang, Kenichi Soga, Jason T. DeJong, Alexandre J. Kabla. Forthcoming. Effects ofbacterial density on growth rate and characteristics of microbial-induced CaCO3 precipitates:a particle-scale experimental study. ASCE Journal of Geotechnical and GeoenvironmentalEngineering. https://doi.org/10.1016/(ASCE)GT.1943-5606.0002509

when bacterial density is high, the formation of $CaCO_3$ follows the ACC-vaterite-calcite sequence as described in Wang *et al.* (2019b).

A supersaturated state is required for $CaCO_3$ precipitation to occur, meaning that the solution has to contain more Ca^{2+} and CO_3^{2-} ions than could normally be dissolved by the solvent. The supersaturation ratio *S* has been used to quantify the level at which supersaturation induces $CaCO_3$ precipitation, which is defined as:

$$S = \frac{[Ca^{2+}] \times [CO_3^{2-}]}{K_{sp}} \quad (5)$$

where $[Ca^{2+}]$ and $[CO_3^{2-}]$ are the concentrations of calcium and carbonate ions, and K_{sp} is the equilibrium $CaCO_3$ solubility product for each experimental temperature (Stumm & Morgan, 1996). A supersaturation ratio that is higher than 1 is required for precipitation to occur.

$CaCO_3$ precipitates can exist as several polymorphs, each of which have different K_{sp} values at different temperatures. At 25 °C, the K_{sp} values of the four main polymorphs of $CaCO_3$ (calcite, aragonite, vaterite, and amorphous $CaCO_3$) are $10^{-8.48}$ M^2, $10^{-8.34}$ M^2, $10^{-7.91}$ M^2 and $10^{-6.40}$ M^2, respectively (Plummer & Busenberg, 1982; Brečevic &Nielsen, 1990). Therefore, when $[Ca^{2+}]\times[CO_3^{2-}]$ is below $10^{-8.48}$ M^2, no precipitation occurs in any forms; when $[Ca^{2+}]\times[CO_3^{2-}]$ is between $10^{-8.48}$ M^2 and $10^{-8.34}$ M^2, only calcite precipitates; when $[Ca^{2+}]\times[CO_3^{2-}]$ is higher than $10^{-6.40}$ M^2, all forms of $CaCO_3$ can precipitate. On the other hand, after the generation of the different forms of $CaCO_3$, when $[Ca^{2+}]\times[CO_3^{2-}]$ drops to below $10^{-6.40}$ M^2 but higher than $10^{-7.91}$ M^2, amorphous (ACC) dissolves whereas the other forms of $CaCO_3$ can remain. When $[Ca^{2+}]\times [CO_3^{2-}]$ drops to between $10^{-8.48}$ M^2 and $10^{-8.34}$ M^2, all forms of $CaCO_3$ dissolve while only calcite remains. When the relatively less stable forms of $CaCO_3$ dissolve, the free Ca^{2+} and CO_3^{2-} can precipitate into the other more stable forms of $CaCO_3$ as long as the supersaturation states are reached. In

To cite:
Yuze Wang, Kenichi Soga, Jason T. DeJong, Alexandre J. Kabla. Forthcoming. Effects ofbacterial density on growth rate and characteristics of microbial-induced CaCO3 precipitates:a particle-scale experimental study. ASCE Journal of Geotechnical and GeoenvironmentalEngineering. https://doi.org/10.1016/(ASCE)GT.1943-5606.0002509

addition, when multiple forms of $CaCO_3$ can precipitate at the same time, the less stable forms of $CaCO_3$ precipitate more quickly than the more stable forms of $CaCO_3$. Therefore, the ACC-vaterite-aragonite-calcite transformation may occur.

During the MICP process, Ca^{2+} ions are normally present at concentrations in the range of 0.1 M-1.5 M from the beginning of the $CaCO_3$ precipitation process, whereas the initial concentration of CO_3^{2-} is zero (Whiffin *et al.*, 2007; van Paassen *et al.*, 2010; Al Qabany & Soga, 2013; Cheng *et al.*, 2017). A diagram illustrating the relationship between phase transformation and the initial supersaturation state is shown in Figure 9. The concentration of Ca^{2+} was assumed to stay constant at 1.0 M. The supersaturation state is dependent on both the hydrolysis of urea, which increases the concentration of CO_3^{2-}, and on the precipitation of $CaCO_3$, which decreases both the concentration of CO_3^{2-} and Ca^{2+}. Because bacterial density affects the bulk ureolysis rate, it also affects the supersaturation state, which in turn influences the formation of different phases of $CaCO_3$. When the bacterial density is low, the concentration of CO_3^{2-}, which is hydrolysed from urea, increases slowly up to the calcite forming line as shown in Figure 9, after which calcite starts forming. When the concentration of CO_3^{2-} is balanced between the forming lines of aragonite and calcite, only calcite can form. Similarly, depending on bacterial density, the other forms of $CaCO_3$ can also either form or not form, depending on whether the supersaturation state of that type of $CaCO_3$ is researched or not. When multiple forms of $CaCO_3$ precipitate, ACC-vaterite-aragonite-calcite transformation may occur.

Bacteria aggregation and crystal aggregation

When the bacterial density is very high (5.2×10^8 cells/ml in this study), bacteria aggregates and crystal aggregates were observed after the first injection of cementation solution (Figure 8). To observe the effect of bacteria aggregates on the formation of $CaCO_3$ crystal aggregates, images of bacteria aggregates and crystal aggregates in the

To cite:
Yuze Wang, Kenichi Soga, Jason T. DeJong, Alexandre J. Kabla. Forthcoming. Effects ofbacterial density on growth rate and characteristics of microbial-induced CaCO3 precipitates:a particle-scale experimental study. ASCE Journal of Geotechnical and GeoenvironmentalEngineering. https://doi.org/10.1016/(ASCE)GT.1943-5606.0002509

same spot of the microfluidic chip are shown in Figure 10. Bacteria aggregates observed after the first injection of cementation solution are shown in Figure 10a. In the same spot, crystal aggregates observed after the 12th injection of cementation solution are shown in Figure 10b. To observe the effect of bacteria aggregates on the formation of $CaCO_3$ crystals in more detail, the magnified images of the squares in Figure 10a taken at 0, 20 min, 1 h and 1 day after the first injection of cementation solution are shown in Figure 10c, and the images taken 24 hours after the 2nd, 3rd, 5th and 7th injections of cementation solution are shown in Figure 10d.

After the first injection of cementation solution, the bacteria aggregated and irregular-shaped $CaCO_3$ crystals formed on the bacteria aggregates (Figure 10c, 0 min image**)**. The bacteria aggregation continued growing, which is shown by the increase in image intensity at 20 min compared with 0 min (Figure 10c, 20 min image). At 20 mins, however, spherical crystals formed on the bacteria aggregates (Figure 10c, 20 min image). The spherical crystals continued growing in size during the first hour after injection (Figure 10c, 1 h image). In addition, more spherical crystals also formed, but not on the bacteria aggregates (Figure 10c, 1 h image). The spherical crystals were not stable and some dissolved by 24 hours after injection (Figure 10c, 1 d image). During the following injections from the 2nd to the 7th, even though more unstable crystals appeared and disappeared, the crystals that were formed on the bacteria aggregates continued growing (Figure 10d). Because the crystals are so close to each other, they merged into one large crystal aggregate as they grew (Figure 10d, 7th injection image).

Crystal aggregates have been observed in many MICP studies (van Paassen 2009; Cheng et al., 2017). This experiment suggests that the crystal aggregates may have formed due to crystal nucleation spots being close to each other. As the crystals grew, they merged into one big aggregate. As the number of bacteria has an effect on the

To cite:
Yuze Wang, Kenichi Soga, Jason T. DeJong, Alexandre J. Kabla. Forthcoming. Effects ofbacterial density on growth rate and characteristics of microbial-induced CaCO3 precipitates:a particle-scale experimental study. ASCE Journal of Geotechnical and GeoenvironmentalEngineering. https://doi.org/10.1016/(ASCE)GT.1943-5606.0002509

number of nucleation sites, more crystals formed when more bacterial cells were present in a given volume. Therefore, the crystals are more likely to be located closer to each other. In addition, because bacteria aggregates contain a high density of bacterial cells, the likelihood of crystals growing on or surrounding them may also be higher than the likelihood for single bacterial cells. In this particular case, the crystal aggregates present within the pores occurred at locations similar to the bacterial aggregates.

Conclusions

In this study, microfluidic chip experiments were conducted to investigate the effects of bacterial density on both the kinetics and characteristics of $CaCO_3$ precipitation at the particle scale. Three bacterial densities (0.6 (low), 2.0 (high) and 5.2×10^8 (very high) cells/ml counted after the first cementation solution injection) were applied in staged injection MICP procedures. Apart from bacterial density, other experimental parameters including the content and concentration of cementation solution, temperature, and injection flow rate of bacterial suspension and cementation solution were kept constant. Both the overall precipitation rate of $CaCO_3$ and the growth rate of individual $CaCO_3$ crystals were quantified. In addition, crystals characteristics in terms of size, number and dissolution processes were analysed. The main findings of the study are summarised as follows.

When bacterial density is a low (0.6×10^8 cells/ml in this study), the crystals form more slowly than in the higher bacterial density cases, but when sufficient time is given (15 hours in this case), the sizes of $CaCO_3$ crystals were the largest among the three cases. The large crystals could be more efficient in bonding sand with larger particles and larger pore sizes. However, the number of $CaCO_3$ crystals produced is low. Improvement in terms of soil strength may require a certain amount of soil particles to be bonded by

To cite:
Yuze Wang, Kenichi Soga, Jason T. DeJong, Alexandre J. Kabla. Forthcoming. Effects ofbacterial density on growth rate and characteristics of microbial-induced CaCO3 precipitates:a particle-scale experimental study. ASCE Journal of Geotechnical and GeoenvironmentalEngineering. https://doi.org/10.1016/(ASCE)GT.1943-5606.0002509

496 $CaCO_3$ crystals. In addition, the time required for $CaCO_3$ to complete the precipitation is
497 long, which implies a long MICP treatment process.
498
499 When bacterial density is high (2.0×10^8 cells/ml in this study), the size of $CaCO_3$ crystals
500 formed might be small and unstable, but over time may transform into larger crystals and
501 more stable forms. The crystals formed at the particle contacts should be big enough to
502 efficiently bond the soil particles, which in turn contributes to the strength and stiffness
503 of MICP treated soils. Therefore, when such a high bacterial density is used, the
504 engineering performance efficiency of MICP-treated soils might be better when a longer
505 treatment duration is applied so that the smaller crystals can reprecipitate into large ones.
506
507 When bacterial destiny is very large (5.2×10^8 cells/ml in this study), the rate of $CaCO_3$
508 precipitation is increased, but this may be due to the formation of large amounts of the
509 unstable form of $CaCO_3$, ACC. Time-dependent transformation of unstable forms of
510 $CaCO_3$ into more stable forms of $CaCO_3$ occurs. ACC has a lower density compared to
511 $CaCO_3$ crystals, and may transport with flow, or be trapped in soil pores. For soils that
512 have small pores, these unstable crystals may locally clog the soil flow paths and affect
513 the homogeneity of MICP treatment.
514
515 High bacterial density (5.2×10^8 cells/ml in this study) also contributes to the formation of
516 bacteria aggregates after the injection of cementation solution, which in turn affects the
517 formation of crystal aggregates. As bacteria aggregates are notably larger compared
518 with individual bacteria, bacteria aggregates might be less likely to become
519 homogenously distributed within the soil matrix, especially when they are large enough
520 to clog the pores which prevents the transport of other bacteria and bacteria aggregates
521 with flow. As the formation of crystal aggregates is affected by bacteria aggregates, a
522 non-homogenous distribution of bacteria within a soil matrix also results in a non-

To cite:
Yuze Wang, Kenichi Soga, Jason T. DeJong, Alexandre J. Kabla. Forthcoming. Effects ofbacterial density on growth rate and characteristics of microbial-induced CaCO3 precipitates:a particle-scale experimental study. ASCE Journal of Geotechnical and GeoenvironmentalEngineering. https://doi.org/10.1016/(ASCE)GT.1943-5606.0002509

523 homogenous distribution of $CaCO_3$. Further work would be useful to investigate the effect
524 of bacterial density on the distribution of bacteria and the resulting effect this has on the
525 distribution of $CaCO_3$ content.
526
527 Based on solubility, calcite is the most stable form of $CaCO_3$ both physically and
528 chemically, and it has been suggested that the precipitation of calcite is preferred for a
529 permanent stable cementation (van Paassen, 2009). Therefore, when designing an
530 MICP treatment protocol, the effects of bacterial density on the phase transformation and
531 the time for crystals to become stable need to be considered. This study suggests that
532 low bacterial density contributes to the production of stable $CaCO_3$ from the beginning,
533 but the precipitation takes longer to complete. High bacterial density leads to precipitation
534 of less stable forms of $CaCO_3$ first, even though the precipitation occurs faster. A longer
535 treatment time is required for $CaCO_3$ to transform from less stable forms to more stable
536 forms.
537
538 The use of microfluidic experiments is useful to assess the ideal bacterial density for
539 various conditions in the field. MICP treatment parameters such as initial bacterial
540 density, bacterial settling time, and injection flow rate of cementation solution all affect
541 the delivered bacterial cell concentration in the soil matrix. Bacterial density directly
542 affects the size and number of $CaCO_3$ crystals formed, which affect the treatment
543 efficiency of MICP for strengthening soils. Correlations between bacterial density and the
544 properties of $CaCO_3$ crystals in terms of number and size from this study could be helpful
545 for the design of MICP treatment protocols for soils with different particle sizes.
546
547 **Data Availability Statement**
548 All data, models, and code generated or used during the study appear in the submitted
549 article.

To cite:
Yuze Wang, Kenichi Soga, Jason T. DeJong, Alexandre J. Kabla. Forthcoming. Effects ofbacterial density on growth rate and characteristics of microbial-induced CaCO3 precipitates:a particle-scale experimental study. ASCE Journal of Geotechnical and GeoenvironmentalEngineering. https://doi.org/10.1016/(ASCE)GT.1943-5606.0002509

Acknowledgements

Y.W. would like to acknowledge Cambridge Commonwealth, European and International Trust, and China Scholarship Council, which collectively funded this project. J.T.D. acknowledges the support of the Engineering Research Center Program of the National Science Foundation under NSF Cooperative Agreement No. EEC-1449501. Any opinions, findings and conclusions or recommendations expressed in this manuscript are those of the authors and do not necessarily reflect the views of the National Science Foundation. The authors would like to thank Dr. David Frost of Georgia Institute of Technology for providing the soil cross sectional image used to design the microfluidic chip. The authors would also like to thank Dr Fedir Kiskin for proofreading this manuscript.

Reference

Al Qabany, A., & Soga, K. (2013). Effect of chemical treatment used in MICP on engineering properties of cemented soils. Géotechnique, 63(4), 331–339.

Al Qabany, A., Soga, K., & Santamarina, C. (2012). Factors Affecting Efficiency of Microbially Induced Calcite Precipitation. Journal of Geotechnical and Geoenvironmental Engineering, 138(8), 992–1001.

Brečević, L., & Nielsen, A. E. (1989). Solubility of amorphous calcium carbonate. J. Cryst. Growth, 98, 504−510.

Chen, G., Hong, Y., & Walker, S. L. (2010). Colloidal and bacterial deposition: Role of gravity. Langmuir, 26(1), 314–319.

Cheng, L., Shahin, M. A., & Mujah, D. (2017). Influence of Key Environmental Conditions on Microbially Induced Cementation for Soil Stabilization. Journal of Geotechnical and Geoenvironmental Engineering, 143(1), 04016083.

DeJong, J. T., Fritzges, M. B., & Nüsslein, K. (2006). Microbially Induced Cementation to Control Sand Response to Undrained Shear. Journal of Geotechnical and Geoenvironmental Engineering, 132(11), 1381–1392

DeJong, J. T., Mortensen, B. M., Martinez, B. C., & Nelson, D. C. (2010). Bio-mediated soil improvement. Ecological Engineering, 36(2), 197–210.

DeJong, J. T., Soga, K., & Kavazanjian, E. (2013). Biogeochemical processes and geotechnical applications: progress, opportunities and challenges. Geotechnique, 63(4), 287–301.

Dunne, W. M. (2002). Bacterial Adhesion: Seen Any Good Biofilms Lately? Clinical Microbiology Reviews. 15(2), 155–166.

Jiang, N.-J., Soga, K., & Kuo, M. (2017). Microbially Induced Carbonate Precipitation for Seepage-Induced Internal Erosion Control in Sand–Clay Mixtures. Journal of Geotechnical and Geoenvironmental Engineering, 143(3), 04016100.

Kim, D. H., Mahabadi, N., Jang J., van Paassen L. A. (2020). Assessing the kinetics and pore-scale characteristics of biological calcium carbonate precipitation in porous medium using a microfluidic chip experiment. Water resources research, 56(2) e2019WR025420

Liu, J., Ford, R. M., & Smith, J. A. (2011). Idling time of motile bacteria contributes to retardation and dispersion in sand porous medium. Environmental Science &Technology, 45(9), 3945–3951.

Lauchnor, E. G., Topp, D. M., Parker, A. E., & Gerlach, R. (2015). Whole cell kinetics of ureolysis by Sporosarcina pasteurii. Journal of Applied Microbiology, 118(6), 1321–1332.

Martinez, B. C., DeJong, J. T., Ginn, T. R., Montoya, B. M., Barkouki, T. H., Hunt, C., & Major, D. (2013). Experimental Optimization of Microbial-Induced Carbonate Precipitation for Soil Improvement. Journal of Geotechnical and Geoenvironmental Engineering, 139(4), 587–598.

To cite:
Yuze Wang, Kenichi Soga, Jason T. DeJong, Alexandre J. Kabla. Forthcoming. Effects ofbacterial density on growth rate and characteristics of microbial-induced CaCO3 precipitates:a particle-scale experimental study. ASCE Journal of Geotechnical and GeoenvironmentalEngineering. https://doi.org/10.1016/(ASCE)GT.1943-5606.0002509

Montoya, B., DeJong, J., & Boulanger, R. (2013). Dynamic response of liquefiable sand improved by microbial-induced calcite precipitation. Géotechnique, 63(4), 302–312.

Persat, A., Nadell, C. D., Kim, M. K., Ingremeau, F., Siryaporn, A., Drescher, K., & Stone, H. A. (2015). The mechanical world of bacteria. Cell, 161(5), 988–997.

Plummer, L. N. & Busenberg, G. E. (1982). The solubilities of calcite, aragonite and vaterite in CO_2–H_2O solutions between 0 and 90 °C and an evaluation of the aqueous model for the system $CaCO_3$–CO_2–H_2O. Geochimica et Cosmochimica Acta, 46, 1011–1040.

Stocks-Fischer, S., Galinat, J. K., & Bang, S. S. (1999). Microbiological precipitation of $CaCO_3$. Soil Biology and Biochemistry, 31(11), 1563–1571.

Stumm, W., Morgan, J. J. (1996). Aquatic chemistry, 3rd edition. New York: Wiley.

Van Paassen, L. (2009). Biogrout: Ground Improvement by Microbially Induced Carbonate Precipitation. PhD Thesis, Delft University of Technology.

Wang, Y., Soga, K. & Jiang, N-J. (2017). Microbial induced carbonate precipitation (MICP): the case for microscale prespective. Proceedings of the 19th International Conference on Soil Mechanics and Geotechnical Engineering, 1099-1102.

Wang Y, Soga K, DeJong J, Kabla A. (2019a). A microfluidic chip and its use in characterizing the particle-scale behaviour of Microbial-Induced Carbonate Precipitation (MICP). Géotechnique, https://doi.org/10.1680/jgeot.18.p.031

Wang Y, Soga K, DeJong J, Kabla A. (2019b). Microscale visualization of Microbial-Induced Carbonate Precipitation (MICP) processes. Journal of Geotechnical and Geoenvironmental Engineering, DOI: 10.1061/(ASCE)GT.1943-5606.0002079

Wang Y (2019). Microbial-Induced Carbonate Precipitation (MICP) from micro to macro scales. PhD Thesis, University of Cambridge, DOI: 10.17863/CAM.35552

Y Wang, C Konstantinou, K Soga, JT DeJong, G Biscontin, AJ Kabla (2020). Enhancing strength of MICP-treated sandy soils: from micro to macro scale, arXiv preprint arXiv:2006.15760

Widdel, F. (2007). Theory and measurement of bacterial growth. Di Dalam Grundpraktikum Mikrobiologie, 1–11.

Whiffin, V. S., van Paassen, L. A., & Harkes, M. P. (2007). Microbial Carbonate Precipitation as a Soil Improvement Technique. Geomicrobiology Journal, 24(5), 417–423.

Zapata, A., & Ramirez-Arcos, S. (2015). A Comparative Study of McFarland Turbidity Standards and the Densimat Photometer to Determine Bacterial Cell Density. Current Microbiology, 70(6), 907–909.

Zhang, W., Ju, Y., Zong, Y., Qi, H., & Zhao, K. (2018). In situ real-time study on dynamics of microbially induced calcium carbonate precipitation at a single-cell level. Environmental Science & Technology, acs.est.8b02660.

Zhao, Q., Li, L., Li, C., Li, M., Amini, F., & Zhang, H. (2014). Factors Affecting Improvement of Engineering Properties of MICP-Treated Soil Catalyzed by Bacteria and Urease. Journal of Materials in Civil Engineering, 26(12), 04014094.

To cite:
Yuze Wang, Kenichi Soga, Jason T. DeJong, Alexandre J. Kabla. Forthcoming. Effects ofbacterial density on growth rate and characteristics of microbial-induced CaCO3 precipitates:a particle-scale experimental study. ASCE Journal of Geotechnical and GeoenvironmentalEngineering. https://doi.org/10.1016/(ASCE)GT.1943-5606.0002509

643 **Table 1** Summary of bacterial, chemical and injection parameters associated with the microfluidic
644 chip experiments

Condition No.	Dilution ratio	Bacterial OD_{600}	Injection number	Injection interval (day)
1	1:14	0.2	12	1
2	1:5	0.5	1	-
3	1:2	1.0	12	1
4	2:1	2.0	1	-
5	1:0	3.0	12	1

645

646 **Table 2** Summary of the changes in bacterial density during MICP treatment

	After BS injection		After settling		After CS injection	
OD_{600} Before injection	Average ($\times 10^8$ cells per ml)	Derived ($\times 10^8$ cells per ml)	Average ($\times 10^8$ cells per ml)	Derived ($\times 10^8$ cells per ml)	Average ($\times 10^8$ cells per ml)	Derived ($\times 10^8$ cells per ml)
0.2	0.95867	0.03186	1.92	0.13	0.56933	0.09581
1.0	3.92333	0.28825	6.09	0.335	2.01333	0.16131
3.0	11.9	0.61644	15.4	0.875	5.212	0.78289

647 Note: BS-bacterial suspension; CS-cementation solution

648

649 **Table 3** Summary of the changes in bacterial density during MICP treatment and associated overall
650 precipitation times

OD_{600} Before injection	Bacterial density ($\times 10^8$ cells per ml)			Overall Precipitation		Reference
	After BS injection	After settling	After CS injection	Time (h)	Rate M/h	
0.2	1	1.9	0.6	15	0.016	P1, this study
1.0	4	6.1	2.0	3	0.083	P3, this study
3.0	12	15.4	5.2	1.5	0.160	P5, this study
1.0	-	-	-	-	0.042	Al Qabany et al., 2012

651

652

653

654

655

To cite:
Yuze Wang, Kenichi Soga, Jason T. DeJong, Alexandre J. Kabla. Forthcoming. Effects ofbacterial density on growth rate and characteristics of microbial-induced CaCO3 precipitates:a particle-scale experimental study. ASCE Journal of Geotechnical and GeoenvironmentalEngineering. https://doi.org/10.1016/(ASCE)GT.1943-5606.0002509

Figure 1 Schematic of the microfluidic chip experiments (Wang et al., 2019a)

Figure 2 (a)Microscope images of one pore at the centre of the microfluidic chip taken at ten minutes after the injection of bacterial suspensions with initial OD_{600} values of 0.2, 0.5, 1.0, 2.0 and 3.0; (b) correlations between the initial OD_{600} of the bacterial suspensions and bacterial density at ten minutes after bacterial injection, cell concentration=$OD_{600}\times4\times10^8$, data are presented as mean ± standard error, and each measurement was repeated three times; (c) image of one pore at the centre of the microfluidic chip taken at 2 hours after the injection of a bacterial suspension with initial OD_{600} values of 0.8 showing bacterial size being about 10 μm; (d) magnified image of middle image of (a) showing bacterial size being about 3 μm in this study

Figure 3 (a) Microscope images of one pore at the centre of the microfluidic chip containing bacterial suspesnions with their intial bacteiral OD_{600} were 0.2, 1.0 and 3.0, taken at ten mins after bacterial injection, after two hours of settling and after the first injection of cementation solution; (b) quantification of bacteiral cencentraion in the images

Figure 4 Ureolysis rate and specific ureolysis rate plotted against bacterial density

Figure 5 (a) Microscope images taken at the centre of the microfluidic chip containing bacterial suspensions at the densities of 0.5, 2.0 and 5.2 $\times10^8$ cell per ml at 0.5, 1, 3 and 24 hours after the first injection of cementation solution; (b) the mean intensity value of the pictures vs. time

Figure 6 (a) Microscope images taken at the centre of the microfluidic chip containing bacterial suspensions at the densities of 0.5, 2.0 and 5.2 $\times10^8$ cell per ml taken at 0.5, 1, 1.5, 2.0, 6, 15 and 24 hours after the first injection of cementation solution; (b) the average crystal volume vs. time in the 1.5 hours plotted and their liner fit; (c) the average crystal volume vs. time in the 24 hours after the first injection of cementation solution

Figure 7 Scatter plot showing the change in the concentration of $CaCO_3$ crystals with time

Figure 8 Microscope images captured at (a) 3h, 6h, 12h, 24h after the first injection of cementation solution, (b) 0h, 3h, 6h, 12h, 24h after the second injection of cementation solution, and (c)24 hours after the completion of the 3^{rd}, 6^{th}, 9^{th} and 12^{th} injection of cementation solution

Figure 9 Scheme illustrating the precipitation-dissolution and phase transformation, assuming the concentration of Ca^{2+} is constantly 1.0 M

Figure 10 (a) Bacteria aggregates formed after the first injection of cementation solution, (b) crystal aggregates aggregate formed 24 hour after the 12^{th} injection of cementation solution, (c) magnified images of the square in Figure 10(a) taken at 0 min, 10 min, 20 min, 1h, 1 day after the 1^{st} injection of cementation solution, (d) magnified images of the square in Figure 10(a) taken at 24 hours after the 2^{nd}, 3^{rd}, 5^{th} and 7^{th} injections of cementation solution

To cite:
Yuze Wang, Kenichi Soga, Jason T. DeJong, Alexandre J. Kabla. Forthcoming. Effects ofbacterial density on growth rate and characteristics of microbial-induced CaCO3 precipitates:a particle-scale experimental study. ASCE Journal of Geotechnical and GeoenvironmentalEngineering. https://doi.org/10.1016/(ASCE)GT.1943-5606.0002509

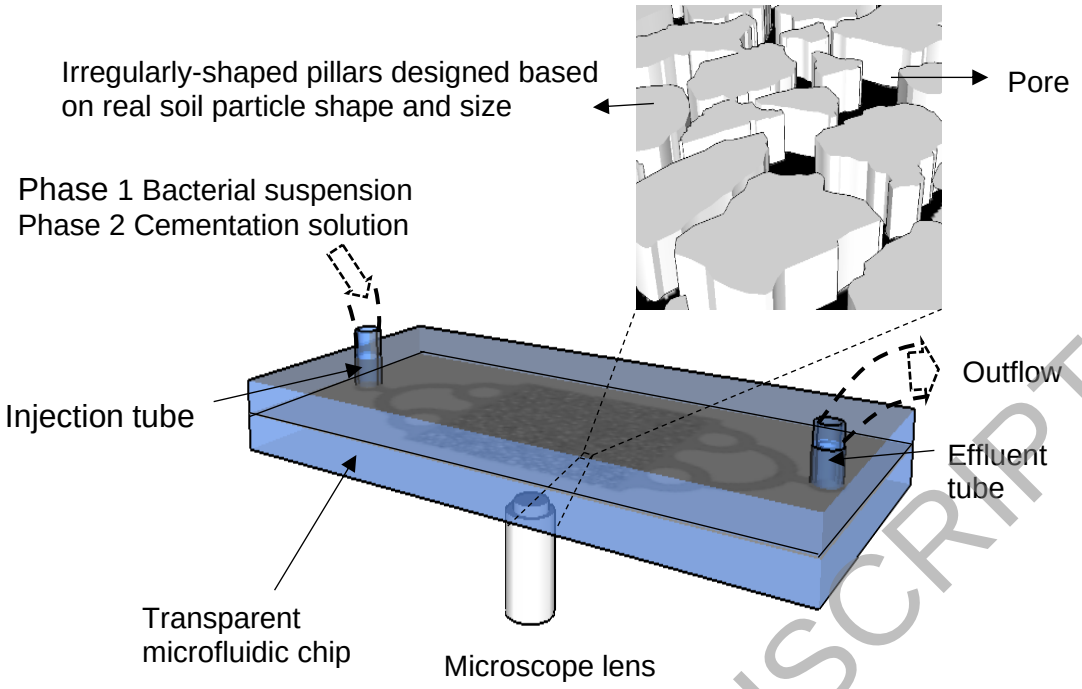

Fig 1

To cite:
Yuze Wang, Kenichi Soga, Jason T. DeJong, Alexandre J. Kabla. Forthcoming. Effects ofbacterial density on growth rate and characteristics of microbial-induced CaCO3 precipitates:a particle-scale experimental study. ASCE Journal of Geotechnical and GeoenvironmentalEngineering. https://doi.org/10.1016/(ASCE)GT.1943-5606.0002509

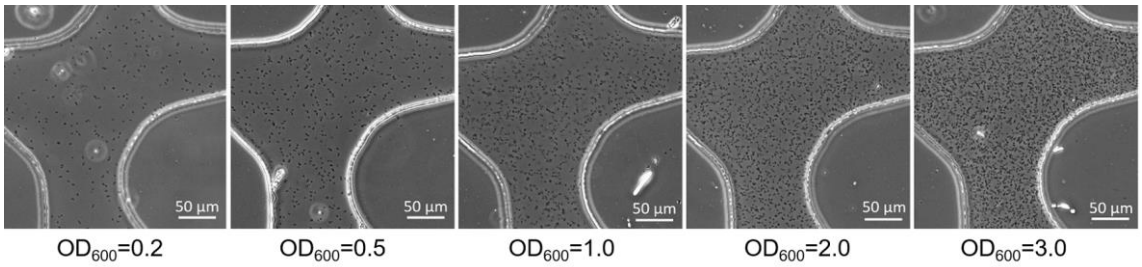

(a)

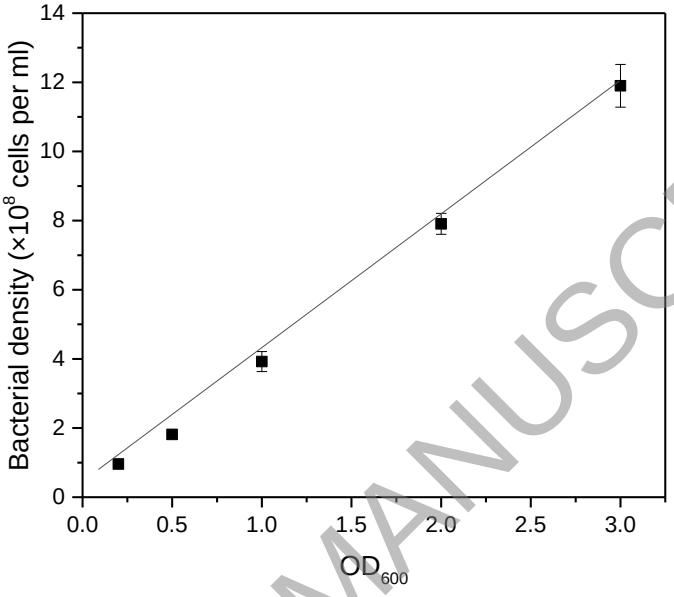

(b)

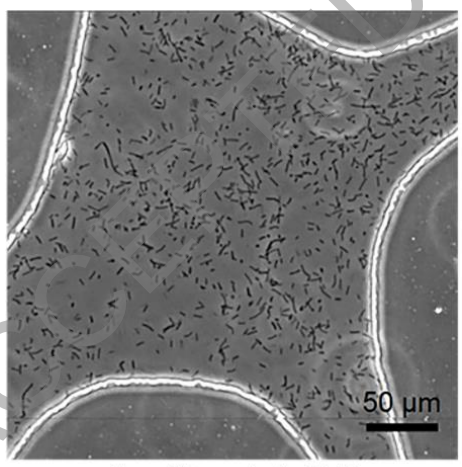

from Wang et al., 2018

(c)

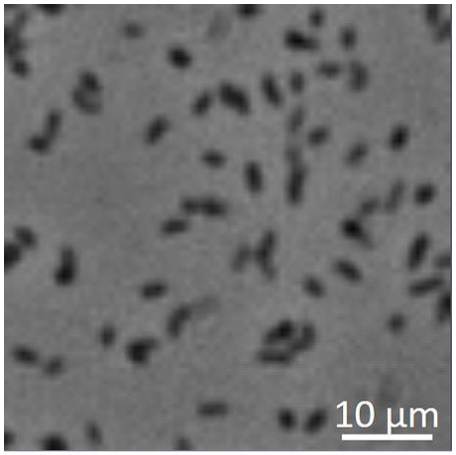

this study

(d)

Fig 2

To cite:
Yuze Wang, Kenichi Soga, Jason T. DeJong, Alexandre J. Kabla. Forthcoming. Effects ofbacterial density on growth rate and characteristics of microbial-induced CaCO3 precipitates:a particle-scale experimental study. ASCE Journal of Geotechnical and GeoenvironmentalEngineering. https://doi.org/10.1016/(ASCE)GT.1943-5606.0002509

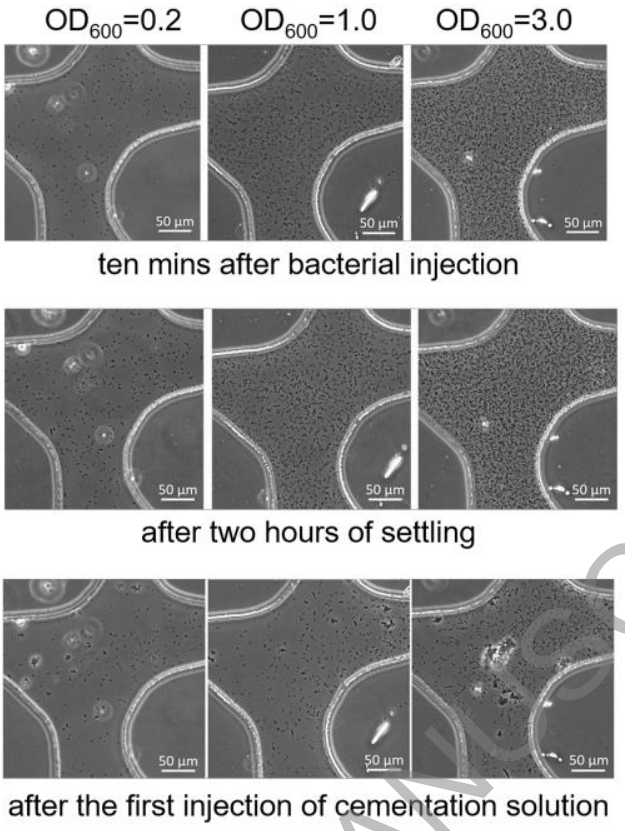

(a)

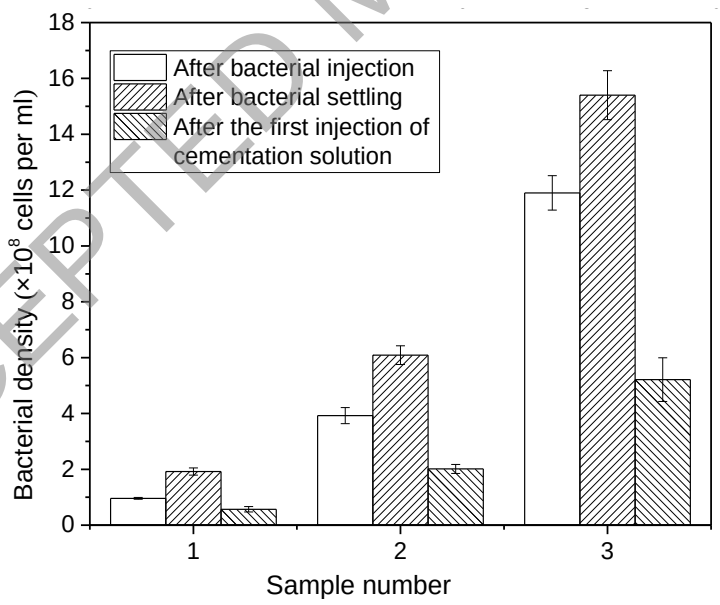

(b)

Fig 3

To cite:
Yuze Wang, Kenichi Soga, Jason T. DeJong, Alexandre J. Kabla. Forthcoming. Effects ofbacterial density on growth rate and characteristics of microbial-induced CaCO3 precipitates:a particle-scale experimental study. ASCE Journal of Geotechnical and GeoenvironmentalEngineering. https://doi.org/10.1016/(ASCE)GT.1943-5606.0002509

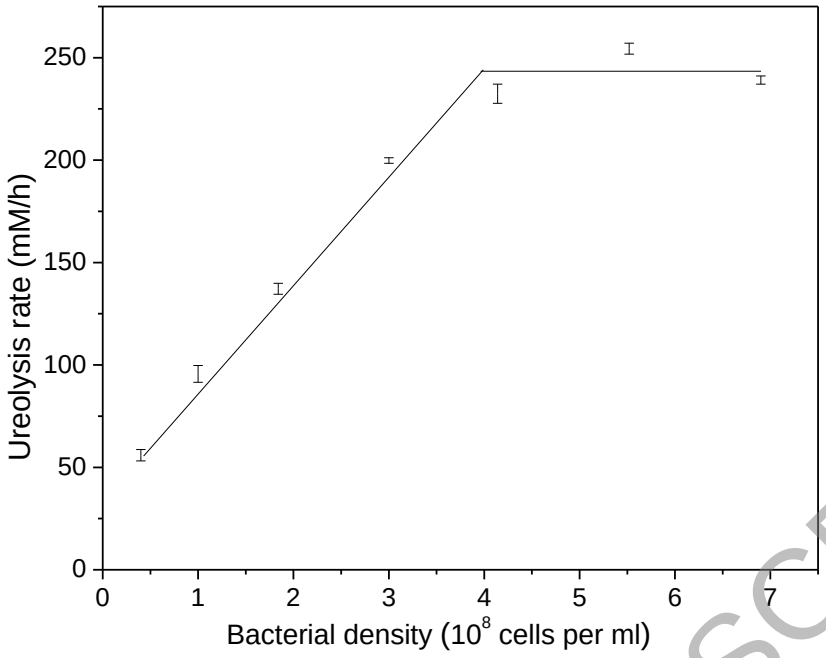

Fig 4

To cite:
Yuze Wang, Kenichi Soga, Jason T. DeJong, Alexandre J. Kabla. Forthcoming. Effects ofbacterial density on growth rate and characteristics of microbial-induced CaCO3 precipitates:a particle-scale experimental study. ASCE Journal of Geotechnical and GeoenvironmentalEngineering. https://doi.org/10.1016/(ASCE)GT.1943-5606.0002509

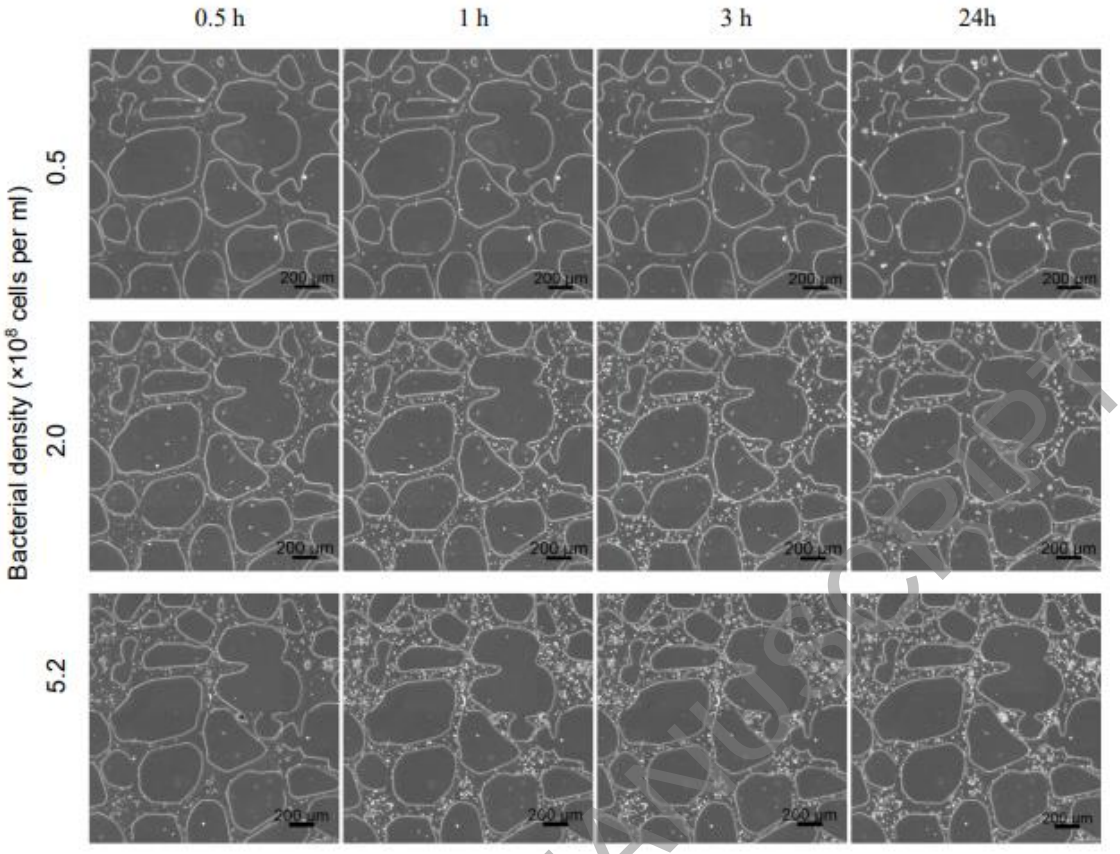

(a)

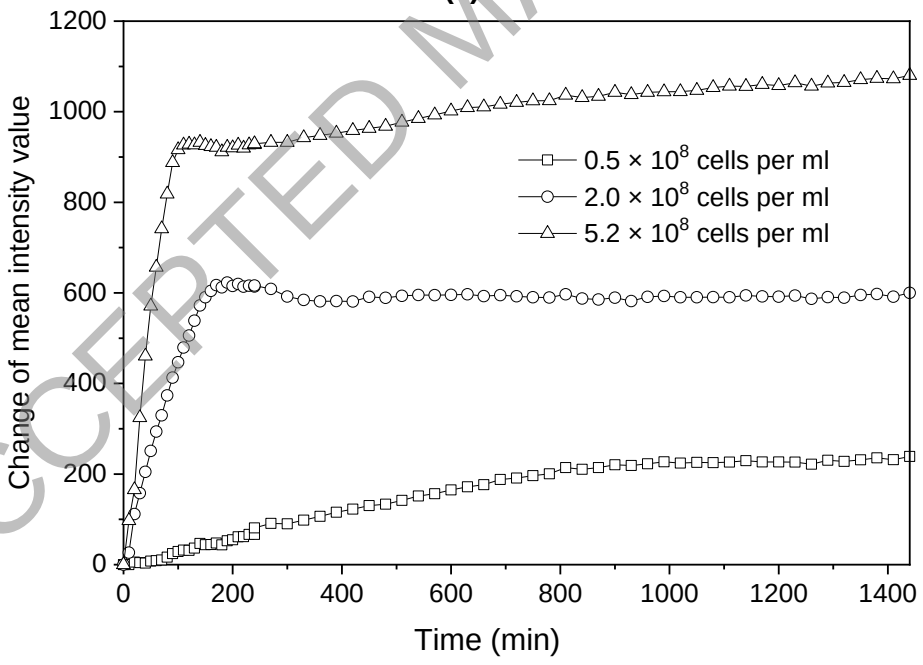

(b)

Fig 5

To cite:
Yuze Wang, Kenichi Soga, Jason T. DeJong, Alexandre J. Kabla. Forthcoming. Effects ofbacterial density on growth rate and characteristics of microbial-induced CaCO3 precipitates:a particle-scale experimental study. ASCE Journal of Geotechnical and GeoenvironmentalEngineering. https://doi.org/10.1016/(ASCE)GT.1943-5606.0002509

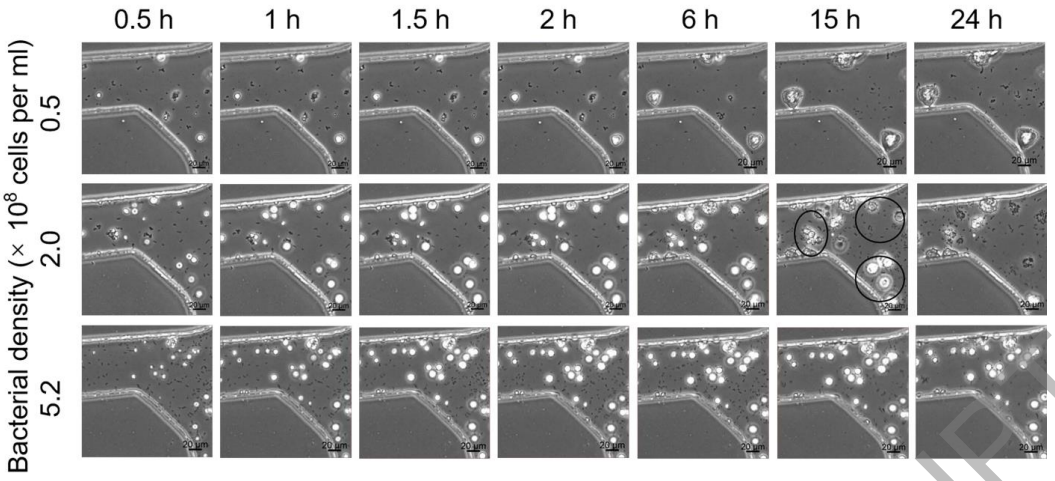

(a)

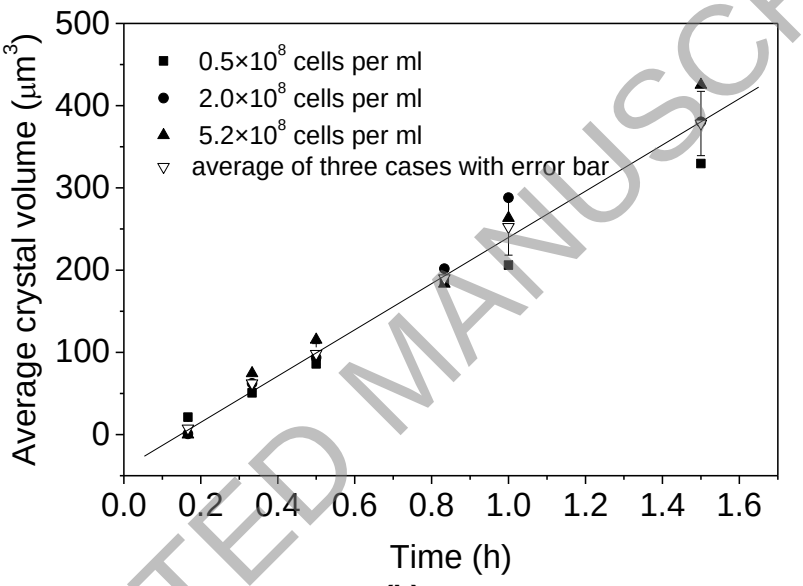

(b)

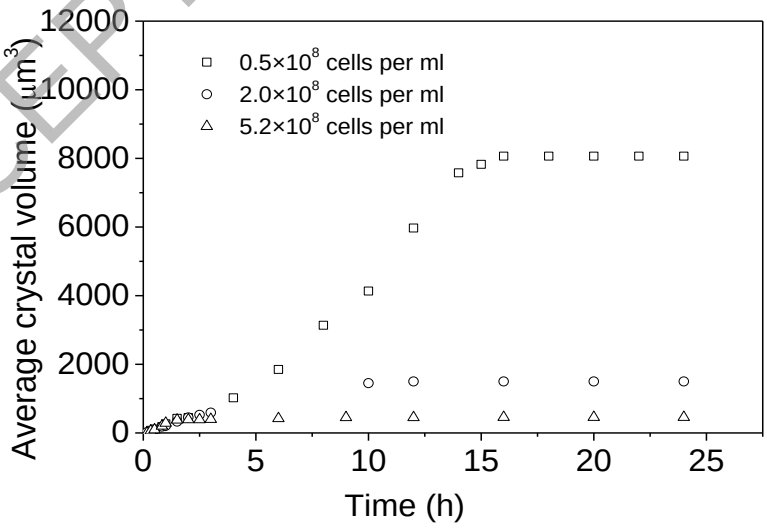

(c)

Fig 6

To cite:
Yuze Wang, Kenichi Soga, Jason T. DeJong, Alexandre J. Kabla. Forthcoming. Effects ofbacterial density on growth rate and characteristics of microbial-induced CaCO3 precipitates:a particle-scale experimental study. ASCE Journal of Geotechnical and GeoenvironmentalEngineering. https://doi.org/10.1016/(ASCE)GT.1943-5606.0002509

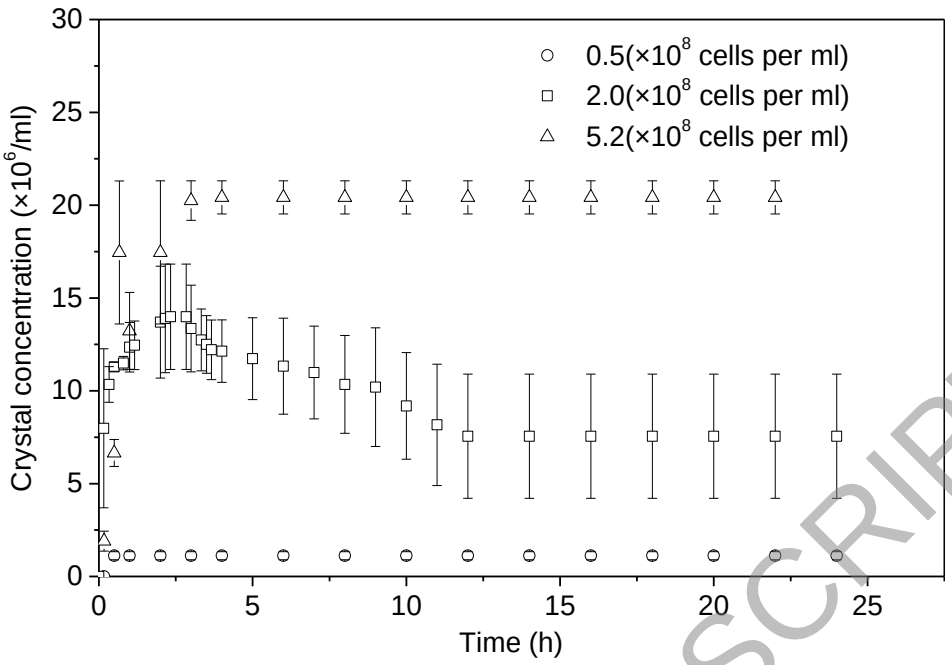

Fig 7

To cite:
Yuze Wang, Kenichi Soga, Jason T. DeJong, Alexandre J. Kabla. Forthcoming. Effects ofbacterial density on growth rate and characteristics of microbial-induced CaCO3 precipitates:a particle-scale experimental study. ASCE Journal of Geotechnical and GeoenvironmentalEngineering. https://doi.org/10.1016/(ASCE)GT.1943-5606.0002509

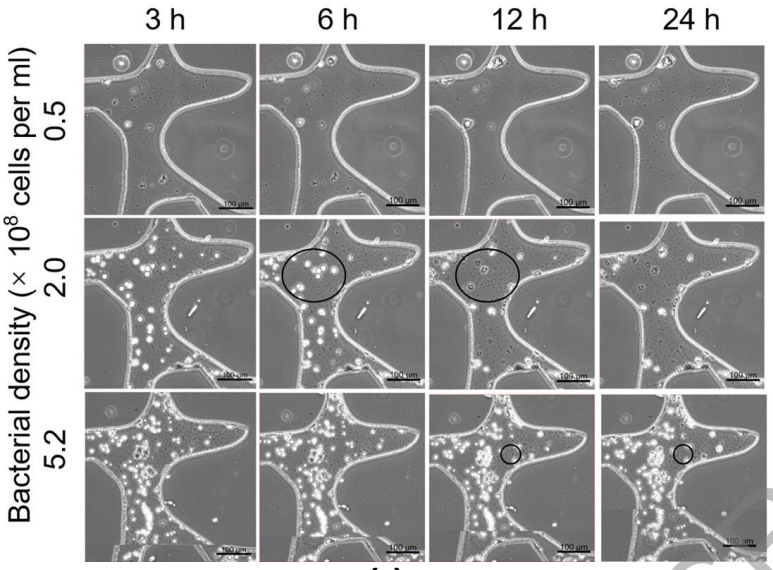

(a)

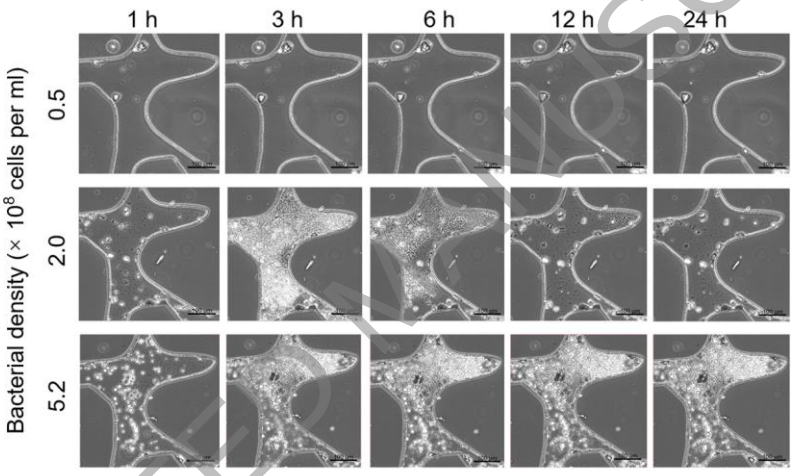

(b)

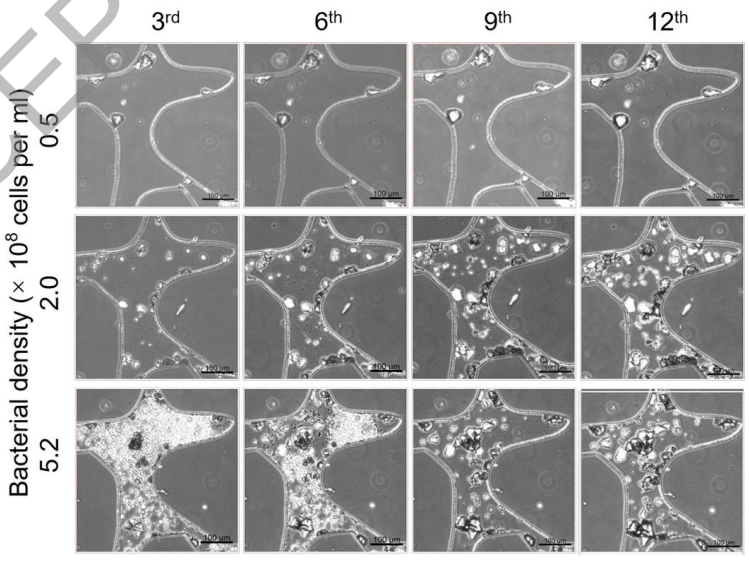

(c)

Fig 8

To cite:
Yuze Wang, Kenichi Soga, Jason T. DeJong, Alexandre J. Kabla. Forthcoming. Effects ofbacterial density on growth rate and characteristics of microbial-induced CaCO3 precipitates:a particle-scale experimental study. ASCE Journal of Geotechnical and GeoenvironmentalEngineering. https://doi.org/10.1016/(ASCE)GT.1943-5606.0002509

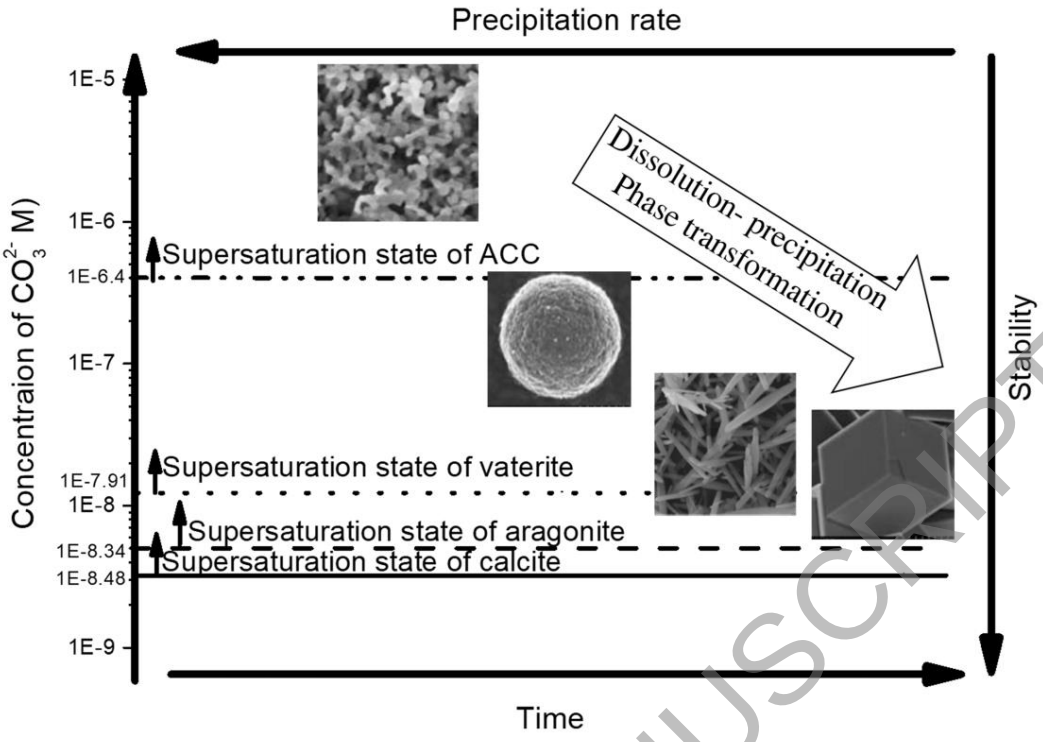

Fig 9

To cite:
Yuze Wang, Kenichi Soga, Jason T. DeJong, Alexandre J. Kabla. Forthcoming. Effects ofbacterial density on growth rate and characteristics of microbial-induced CaCO3 precipitates:a particle-scale experimental study. ASCE Journal of Geotechnical and GeoenvironmentalEngineering. https://doi.org/10.1016/(ASCE)GT.1943-5606.0002509

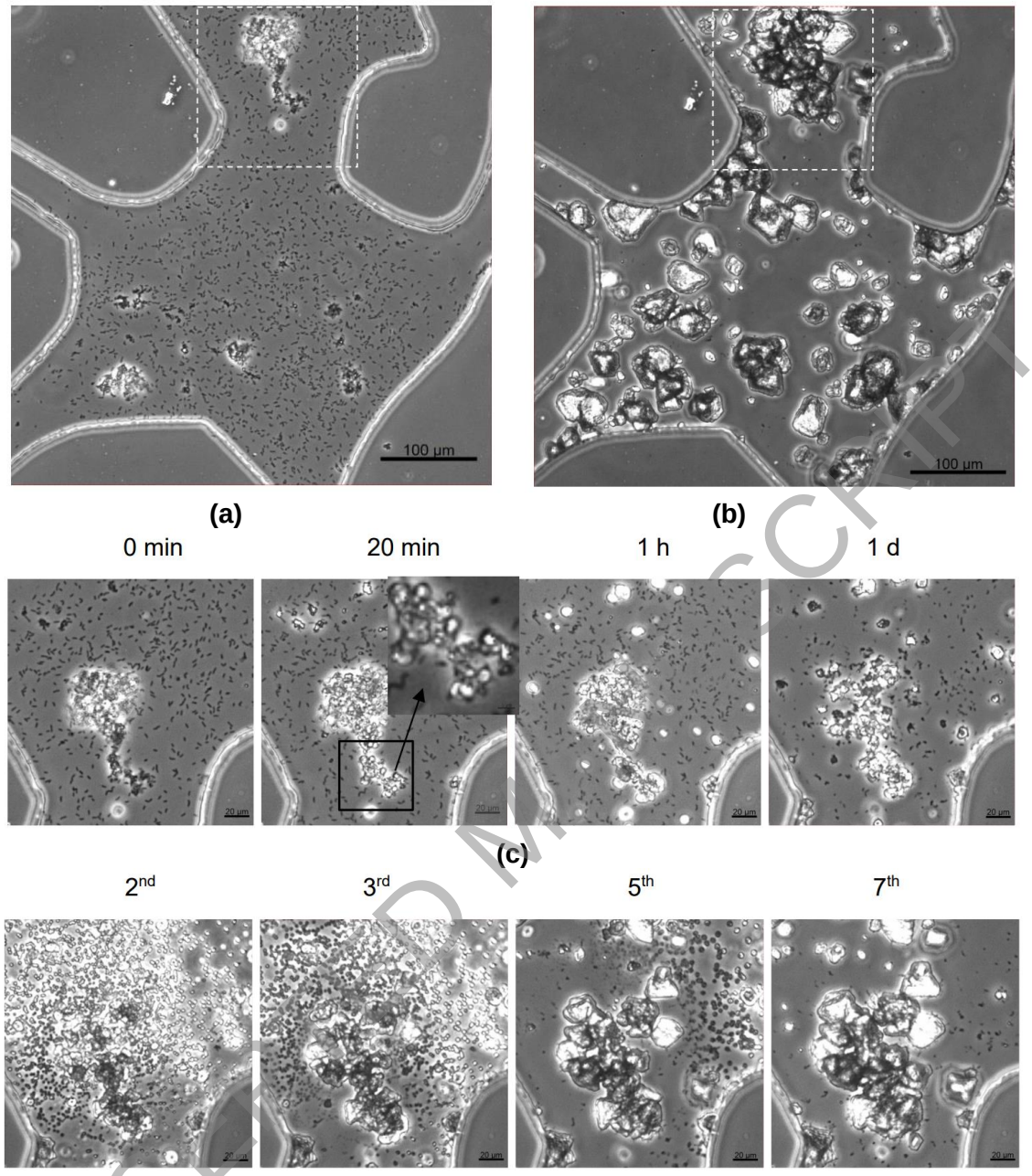

Fig 10